J|A|C|S ARTICLES

Published on Web 09/29/2009

Interaction of ClO Radical with Liquid Water

Shiyu Du,[†] Joseph S. Francisco,*[,†] Gregory K. Schenter,[‡] and Bruce C. Garrett[‡]

Department of Chemistry and Department of Earth and Atmospheric Sciences, Purdue University, West Lafayette, Indiana 47907-1393, and Fundamental & Computational Sciences Directorate, Pacific Northwest National Laboratory, Richland, Washington 99352

Received April 27, 2009; E-mail: francisc@purdue.edu

Abstract: In the present work, the interaction between ClO radical and liquid water is studied using molecular dynamics simulations. We perform simulations of collisions of a ClO radical with the surface of liquid water to understand the accommodation of ClO by liquid water. Simulation results show that the ClO radical has a higher propensity to be adsorbed on the air−water interface than to be dissolved in the bulk. The free energy profile is also calculated, and the solvation free energy and Henry's law constant are determined for ClO as ΔG_s of −2.9 kcal/mol and 5.5 M/atm, respectively. The mechanism of the ClO recombination reaction is also discussed, and the results are consistent with laboratory findings.

I. Introduction

The ClO radical plays a critical role in stratospheric destruction of ozone.[1−7] One set of reactions that are central to how ozone is destroyed is as follows:

$$ClO\cdot + ClO\cdot + M \rightarrow Cl_2O_2 + M \quad (1)$$

$$Cl_2O_2 + h\nu \rightarrow Cl\cdot + ClOO\cdot \quad (2)$$

$$ClOO\cdot + M \rightarrow Cl\cdot + O_2 + M \quad (3)$$

$$Cl\cdot + O_3 \rightarrow ClO\cdot + O_2 \quad (4)$$

The net reaction is $2O_3 \rightarrow 3O_2$ catalyzed by the ClO radical. In this process, the formation and the photodecomposition of the ClO dimer (Cl_2O_2) are essential to the chemistry. However, recent studies have suggested that this gas-phase chemistry alone cannot account for ozone loss due to chlorine-catalyzed loss of ozone.[8] Farman et al.[9] discovered large reductions in the abundance of total column of ozone over the Antarctic in the late winter and early spring. During these periods, field observations showed that elevated ClO radicals are confined to the Antarctic vortex, where the temperatures are cold enough to form polar stratospheric clouds (PSCs). These clouds were previously believed to be ice, but subsequent studies have shown that polar stratospheric clouds are quasi-liquid.[10,11] Reactions on the surface of PSCs are known to occur,[12−14] but little is known about the role of the chemistry of ClO radicals on these cloud surfaces. The influence of water is an important factor for understanding ClO chemistry in the atmosphere. Francisco and Sander[15] showed that water can act as a chaperone in the ClO recombination reaction in the gas phase. The key species involved in the chemistry is the $ClO\cdot H_2O$ radical−molecule complex. The $ClO\cdot H_2O$ complex has also been the subject of several previous studies.[15−18] Two different minima in the potential energy surface (PES) of the complex have been found by ab initio calculations. It is also found that a low-lying excited state exists.[17,18]

To gain insight into chemical reactions of ClO radicals in the presence of high abundance of water molecules in a cloudy atmosphere, it is necessary to understand the physicochemical character of ClO radicals in an aqueous environment. However, most studies of the ClO radical have been performed in the gas phase, and the influence of interactions in liquid water on the chemistry of ClO radicals in the atmosphere is not understood. Furthermore, even the uptake of ClO radicals at the surface of liquid water has not been previously studied. The recent study of Knipping et al.[5] demonstrates just how important the uptake and reaction of radical species such as OH with aqueous liquid particles are in the atmosphere and in atmospheric reaction mechanisms.

[†] Purdue University.
[‡] Pacific Northwest National Laboratory.

(1) Anderson, J. G.; Brune, W. H.; Toohey, D. W. *Science* **1991**, *251*, 39.
(2) Solomon, P. M.; Connor, B.; de Zafra, R. L.; Parrish, A.; Barrett, J.; Jaramillo, M. *Nature* **1987**, *328*, 411.
(3) Tung, K. K.; Ko, J. K. W.; Rodriguez, J. M.; Sze, N. D. *Nature* **1986**, *322*, 811.
(4) Cox, R. A.; Hayman, G. D. *Nature* **1988**, *332*, 796.
(5) Knipping, E. M.; Lakin, J. J.; Foster, K. L.; Jungwirth, P.; Tobias, D. J.; Gerber, R. B.; Dabdub, D.; Finlayson-Pitts, B. J. *Science* **2000**, *288*, 301.
(6) Molina, M. J. *Science* **1987**, *238*, 1253.
(7) Sander, S. P.; Friedl, R. R.; Yung, Y. L. *Science* **1989**, *245*, 1095.
(8) Pope, F. D.; Hansen, J. C.; Bayes, K. D.; Friedl, R. R.; Sander, S. P. *J. Phys. Chem. A* **2007**, *111*, 4322.
(9) Farman, J. C.; Gardiner, B. G.; Shankin, J. D. *Nature* **1985**, *315*, 207.
(10) Koop, T.; Biermann, U. M.; Raber, W.; Luo, B. P.; Crutzen, P. J.; Peter, T. *Geophys. Res. Lett.* **1995**, *22*, 917.
(11) Tabazadeh, A.; Turco, R. P.; Drdla, K.; Jacobson, M. Z.; Toon, O. B. *Geophys. Res. Lett.* **1994**, *21*, 1619.
(12) Solomon, S.; Garcia, R. R.; Rowland, F. S.; Wuebbles, D. J. *Nature* **1986**, *321*, 755.
(13) McElroy, M. B.; Salawitch, R. J.; Wofsy, S. C.; Logan, J. A. *Nature* **1986**, *321*, 759.
(14) Crutzen, P. J.; Arnold, F. *Nature* **1986**, *324*, 651.
(15) Francisco, J. S.; Sander, S. P. *J. Am. Chem. Soc.* **1995**, *117*, 9917.
(16) Li, Y.; Francisco, J. S. *J. Chem. Phys.* **2001**, *115*, 8381.
(17) Du, S.; Francisco, J. S.; Schenter, G. K.; Iordanov, T. D.; Garrett, B. C.; Dupuis, M.; Li, J. *J. Chem. Phys.* **2006**, *124*, 224318.
(18) Fu, H.; Zhou, Z.; Zhou, X. *Chem. Phys. Lett.* **2003**, *382*, 466.

10.1021/ja9033186 CCC: $40.75

Table 1. Refined Parameters for the ClO·H_2O Complex[a]

parameter (unit)	value
q_{Cl} (10^{-20} C)	4.56
q_O (10^{-20} C)	–4.56
ε_{OO} (kcal/mol)	0.386
σ_{HO} (Å)	2.117
ε_{HO} (kcal/mol)	0.220
σ_{OCl} (Å)	2.673
ε_{OCl} (kcal/mol)	0.502
ε_{HCl} (kcal/mol)	0.091
n_{OCl}	12.0
m_{OCl}	6.0
n_{HCl}	9.01
m_{HCl}	4.51

[a] n_{xy} and m_{xy} (xy = OCl, HO, and HCl) are exponents in the Lennard-Jones-type interactions, that is, $4\varepsilon_{xy}[(\sigma_{xy}/r_{xy})^{n_{xy}} - (\sigma_{xy}/r_{xy})^{m_{xy}}]$, where r_{xy} is the interatomic distance between atom x on water and atom y on ClO.

The lack of similar information for the important ClO radical stresses the importance of studies to gain knowledge about the uptake and chemistry of ClO radical on liquid water.

This work focuses on a study of the interaction between ClO radical and liquid water using molecular dynamics (MD) simulation. The purpose of this work is to study the surface uptake and distribution of the ClO radical on water to provide insight into the corresponding impact on the ClO reaction mechanism.

II. Computational Methods

In this work, classical MD simulations are performed with the modified Thole-type model (mTTM) for the ClO·H_2O system, which was constructed on the basis of the TTM2-R water model.[17,19−23] In the mTTM model, the electrostatic interactions are calculated using the Thole-type charge distribution. The potential of the ClO radical and H_2O molecule is calculated by the following equation:

$$U_{tot} = U_{elec} + U_{pair} + U_{ind} \quad (5)$$

where U_{tot} is the total potential energy of the system, U_{elec} is the electrostatic potential, U_{pair} is the Lennard-Jones-type pairwise potential, and U_{ind} is the induction energy. The functional form of each component in eq 5 is given elsewhere.[17,23] The potential was partially reparameterized to make the local minimum geometry agree better with the prediction of high level ab initio calculations. The level of theory is the same as used previously to construct the mTTM potential: the all-electron coupled cluster method including single and double excitations with a perturbation estimation of the triple excitations[24−27] with the augmented correlation-consistent polarized valence triple-ζ[28,29] [CCSD(T)/aug-cc-pVTZ] basis set. The new ground-state parameters are shown in Table 1. All other parameters are the same as the ClO·H_2O ground-state potential reported previously.[23] Because the purpose of this work is to understand the impact of water molecules on the relative reactivity of the ClO radical in the aqueous solution and how the ClO interacts with adjacent water molecules, it is important to have geometries of the minima that are as accurate as possible. The optimized geometries of the ClO·H_2O systems including the ab initio, original mTTM, and refined mTTM predictions are shown in Figure 1. The binding energies of the two minima are 3.46 and 3.06 kcal/mol with the refined mTTM model, respectively. Although the error of the binding energies relative to the ab initio data (3.42 and 3.22 kcal/mol) and the geometry of the global minimum does not change with the new parameters, it can be clearly seen that the geometric parameters for the local minimum are greatly improved for the ground state.

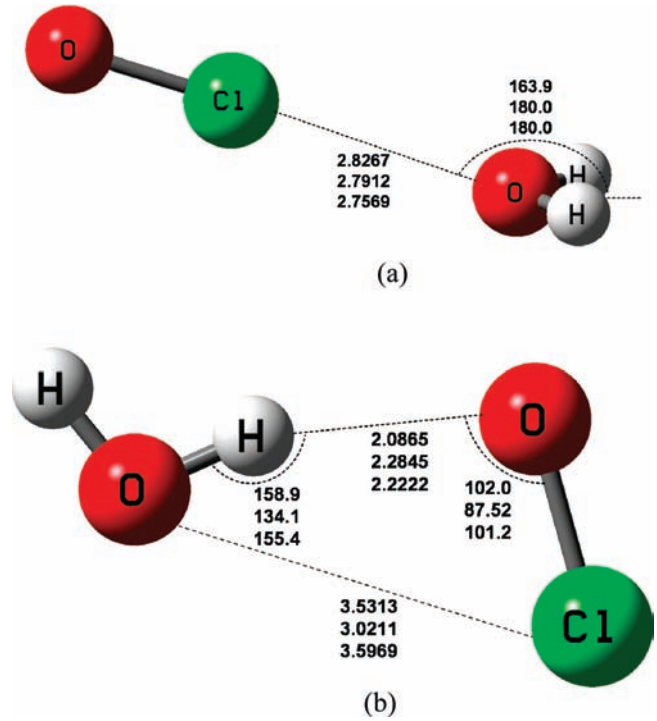

Figure 1. The geometry parameters of ClO·H_2O optimized structures. The values listed from top to bottom are predicted with the methods of CCSD(T), the original mTTM, and refined mTTM. Distances are in angstroms, and angles are in degrees. (a) Global minimum; (b) local minimum.

In our simulations, the interaction between water molecules is calculated with the TTM2-R model, and the refined ground state mTTM is used in the interaction between a ClO radical and water molecules. The force in the MD simulation is calculated classically, that is, by $\vec{F}_i = -\nabla_{r_i} U_{tot}$, where F_i is the force acting on atom i and r_i denotes the gradient is carried out respective to the coordinates of atom i. The liquid/vapor interface of water is represented here by a water slab comprised of 550 H_2O molecules in a simulation box that is an elongated cell with dimension of 24.9 Å × 24.9 Å × 74.9 Å. The simulations employ periodic boundary conditions and are performed with the canonical constant-volume (NVT) ensemble. We also perform simulations of ClO in bulk liquid using a cubic arrangement of 550 H_2O molecules with periodic boundary conditions in an isobaric (NPT) ensemble. The purpose of the bulk NPT simulations is to discover the behavior of ClO radicals when dissolved in water under atmospheric conditions and to compare the results from these simulations using those from simulations of the slab geometry with an NVT ensemble. All of the simulations except the scattering calculations, which are described below, are performed for at least 400 ps with approximately 50 ps equilibrium time. The equilibrium time is the same as that used in previous simulations of pure water with the TTM2-R model.[23] The employed

(19) Burnham, C. J.; Li, J. C.; Xantheas, S. S.; Leslie, M. *J. Chem. Phys.* **1999**, *110*, 4566.
(20) Burnham, C. J.; Xantheas, S. S. *J. Chem. Phys.* **2002**, *116*, 1479.
(21) Xantheas, S. S.; Burnham, C. J.; Harrison, R. J. *J. Chem. Phys.* **2002**, *116*, 1493.
(22) Burnham, C. J.; Xantheas, S. S. *J. Chem. Phys.* **2002**, *116*, 1500.
(23) Du, S.; Francisco, J. S.; Schenter, G. K.; Garrett, B. C. *J. Chem. Phys.* **2007**, *126*, 114304.
(24) Hampel, C.; Werner, H.-J. *J. Chem. Phys.* **1996**, *104*, 6286.
(25) Raghavachari, K.; Trucks, G. W.; Pople, J. A.; Head-Gordon, M. *Chem. Phys. Lett.* **1989**, *157*, 479.
(26) Scuseria, G. E. *Chem. Phys. Lett.* **1991**, *176*, 27.
(27) Knowles, P. J.; Hampel, C.; Werner, H. J. *Chem. Phys.* **1993**, *99*, 5219.
(28) Kendall, R. A.; Dunning, T. H., Jr.; Harrison, R. J. *J. Chem. Phys.* **1992**, *96*, 6796.
(29) Woon, D. E.; Dunning, T. H., Jr. *J. Chem. Phys.* **1993**, *98*, 1358.

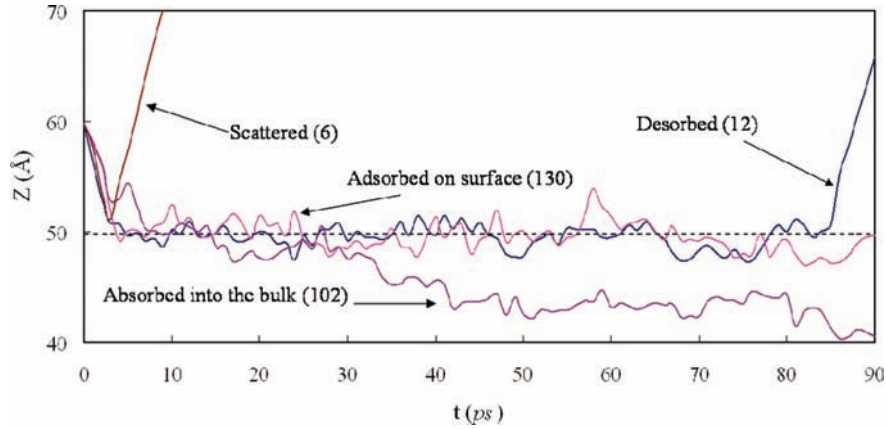

Figure 2. The scattering plot of one ClO radical on the air−water interface. The trajectories are sampled from each type of scattering result.

step size is 1.0 fs. The step size is reduced to 0.5 fs when it is necessary to get a more accurate sampling of the 12−10−6 pairwise potential for the H_2O-H_2O interaction. In the calculation, the long-range electrostatic force is calculated with the Particle Meshed Ewald (PME)[30,31] summations with the radial cutoff value of 9 Å. The short-range force is calculated with the mTTM and TTM2-R model as described with a 7 Å cutoff. All of the simulations in this work are performed at 298.15 K. The adopted thermostat to control the constant temperature in the dynamics is the Nose−Hoover chain.[32,33] The weak-coupling method[34] is used to control constant pressure in the calculation of NPT ensemble. Because both TTM2-R and mTTM are rigid models, the internal coordinates of each molecule are constrained by the SHAKE[35] algorithm in the simulations. All of the simulations are performed with a modified version of the AMBER 7 program package[36] in which our mTTM and the TTM2-R potentials are embedded.

III. Results and Discussion

The first study performed is the scattering of a ClO radical off the surface of liquid water. In the calculations, the ClO radical is originally positioned 10.0 Å above the surface. The initial velocity of ClO is randomly assigned by the Maxwell distribution at 298.15 K with the *Z* component toward the water bulk. A total number of 250 simulations are examined in this work, with the simulation time of 90 ps for each trajectory. The simulation time is the same as that used by Roeselová et al.[37] in their study of the surface accommodation of OH radical at the air/water interface. The *Z* component of ClO trajectories sampled from four types of scattering consequences is given in Figure 2. As shown in the figure, within the simulation time, 102 trajectories have the ClO radical absorbed inside the water bulk, 130 have ClO staying on the air−water interface, 6 are scattered, and 12 are desorbed. The thermal accommodation coefficient, *S*, is defined as the fraction of molecules that collide with the surface that result in thermal accommodation at the interface. The mass accommodation coefficient (α) is defined as the ratio of the number of gas molecules incorporated into the liquid relative to the number of molecules impinging on the liquid phase. Using an analysis of the trajectory results proposed by Roeselová et al.[37] gives a thermal accommodation coefficient (*S*) of 0.93 [1.0 − (6 + 12)/250 = 0.93] and a microscopic mass accommodation coefficient (α) of 0.85 [1.0 − (6 + 12)/(6 + 12 + 102) = 0.85], respectively. These parameters qualitatively indicate that the ClO radical has a high tendency to stick to a water surface.

From a microscopic point of view, a mass accommodation coefficient close to unity is not surprising, because the $ClO\cdot H_2O$ binding energy, calculated to be 3.42 kcal/mol, exceeds the translational energy of thermal scattering at $T = 298$ K ($k_BT \approx$ 0.6 kcal/mol). Previous MD studies for hydrogen-bonding systems generally predict that the thermal collisions result in nearly unit mass accommodation coefficients.[38−44] However, the MD determined mass accommodation coefficients are upper bound values, because it is possible that the time for some of the desorption events to occur may be longer than the scattering time. So our studies provide an upper bound to the mass accommodation coefficient for ClO on water. When we compare the binding energy of $OH\cdot H_2O$[17] (5.8 kcal/mol) to that of $ClO\cdot H_2O$, the binding energies suggest that the mass accommodation for $OH\cdot H_2O$ and $ClO\cdot H_2O$ should be comparable. Indeed, the computed value of $\alpha_{OH} = 0.83$[37] at 300 K is comparable to $\alpha_{ClO} = 0.85$ at 298.15 K. All previous experimental heterogeneous studies of ClO looked at ClO on ice, nitric acid trihydrate (NAT) surfaces, and sulfuric acid surfaces at low temperature (e.g., 183 or 213 K). These experiments estimated an uptake coefficient (γ) for ClO. These uptake coefficients are small (i.e., γ[45] ≈ 0.01 and γ[46,47] $< 10^{-4}$) for ClO on ice and doped ice. As discussed elsewhere,[48] the

(30) Essmann, U.; Perera, L.; Berkowitz, M. L.; Darden, T.; Lee, H.; Pedersen, L. G. *J. Chem. Phys.* **1995**, *103*, 8577.
(31) Darden, T.; York, D.; Pederson, L. *J. Chem. Phys.* **1993**, *98*, 10089.
(32) Evans, D. J.; Holian, B. L. *J. Chem. Phys.* **1985**, *83*, 4069.
(33) Martyna, G. J.; Klein, M. L.; Tuckerman, M. *J. Chem. Phys.* **1992**, *97*, 2635.
(34) Berendsen, H. J. C.; Postma, J. P. M.; van Gunsteren, W. F.; DiNola, A.; Haak, J. R. *J. Chem. Phys.* **1984**, *81*, 3684.
(35) Ryckaert, J. P.; Ciccotti, G.; Berendsen, H. C. *J. Comput. Phys.* **1977**, *23*, 327.
(36) Case, D. A.; *AMBER 7*; University of California: San Francisco, 1999.
(37) Roeselová, M.; Vieceli, J.; Dang, L. X.; Garrett, B. C.; Tobias, D. J. *J. Am. Chem. Soc.* **2004**, *126*, 16308.
(38) Taylor, R. S.; Garrett, B. C. *J. Phys. Chem. B* **1999**, *103*, 844.
(39) Morita, A.; Sugiyama, M.; Kameda, H.; Koda, S.; Hanson, D. R. *J. Phys. Chem. B* **2004**, *26*, 9111.
(40) Wilson, M. A.; Pohorille, A. *J. Phys. Chem. B* **1997**, *101*, 3130.
(41) Morita, A. *Chem. Phys. Lett.* **2003**, *375*, 1.
(42) Vieceli, J.; Roeselová, M.; Potter, N.; Dang, L. X.; Garrett, B. C.; Tobias, D. J. *J. Phys. Chem. B* **2005**, *109*, 15876.
(43) Vieceli, J.; Roeselová, M.; Tobias, D. J. *Chem. Phys. Lett.* **2004**, *393*, 249.
(44) Kassianov, E. I.; Barnard, J. C.; Ackerman, T. P. *J. Geophys. Res.* **2004**, *109*, D09201.
(45) Leu, M. T. *Geophys. Res. Lett.* **1988**, *15*, 851.
(46) Kenner, R. D.; Plumb, I. C.; Ryan, K. R. *Geophys. Res. Lett.* **1993**, *20*, 193.
(47) Abbatt, J. P. D. *Geophys. Res. Lett.* **1996**, *23*, 1681.
(48) Garrett, B. C.; Schenter, G. K.; Morita, A. *Chem. Rev.* **2006**, *106*, 1355.

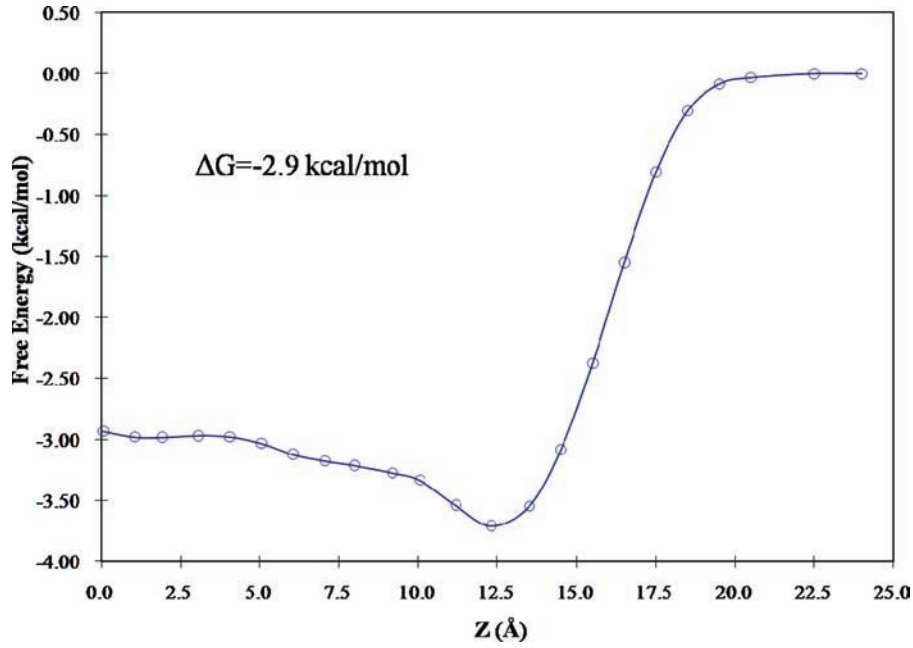

Figure 3. The free energy profile calculated by the PMF method. The point with $Z = 0.0$ corresponds to the middle of the water slab. The ΔG_s value is calculated by eq 6.

relationship between microscopic mass accommodation coefficients determined from simulations and experimental uptake coefficients and mass accommodation coefficients is not well established. This fact, as well as the different phases and different temperatures, make it difficult to directly compare the experimental uptake coefficients and our calculated mass accommodation coefficient.

In the atmosphere, the liquid water in water droplets or aerosols can behave as a transportation media of free radicals, so it is important to understand the thermodynamic equilibrium between ClO radicals in the gas phase and in liquid water. This information has not been reported in the literature of ClO radical. In this work, we performed free energy calculation using the Potential of Mean Force (PMF) method.[49] According to the PMF method, the free energy can be obtained by using the following formula:

$$\Delta G = \int_{Z_o}^{Z_s} -\langle \vec{F}(Z) \rangle \, dz \tag{6}$$

where ΔG is the Gibbs free energy difference to move a molecule from a position with the Z component of Z_0 to any position with Z_s. $\langle F(z) \rangle$ is the time averaged force acting on the molecule of interest, that is, ClO radical. The free energy of solvation (ΔG_s) is calculated by moving the radical from a position infinitely far from the air−water interface to the center of the water bulk and integrating the mean force at each position along the path. The mean force of the radical at each Z value is calculated by constraining the Z component of the radical and averaging the force over at least 400 ps. The resulting PMF is shown in Figure 3. It can be seen from the figure that the free energy has a minimum at the water−air interface, which means that the thermodynamically most stable configuration has the ClO radical accommodated on the surface of liquid water. The curve shown in Figure 3 is constant to within statistical uncertainty from $Z = 0$ to ~5 Å. When $Z = 5-8$ Å, the systematic decrease in free energy may be due to the fact that the ClO radical has a long bond length (1.36 A),[23] which may cause larger perturbations and more long-range effects on water molecules than smaller radicals such as OH radicals. Consequently, there is a surfactant effect that starts to occur when the ClO radical is 7 Å from a water surface. The magnitude of the interfacial minimum in the PMF at ~12.5 Å is larger than the statistical uncertainty. A better estimate of numerical error in the PMF would be obtained by also calculating it starting in the bulk water and moving to the vapor; however, it would not change the qualitative feature of this curve, which clearly shows there is appreciable probability for ClO to be found at the interface.

The ΔG_s value for the bulk solvation of the ClO radical according to our calculations is −2.9 kcal/mol. This value is 1 kcal/mol lower than that of OH radical, −3.9 kcal/mol.[37,50,51] This is a result of the lower binding energy for $ClO \cdot H_2O$ than $OH \cdot H_2O$ radical−molecule complexes. The standard solvation free energy (ΔG_s^0) with the standard condition of $p_0 = 1$ atm for pressure and $c_0 = 1$ M of concentration is obtained by:[52]

$$\Delta G_s^0 = \Delta G_s + RT \ln(RTc_0/p_0) \tag{7}$$

The Henry's law constant (k_H) defined as the ratio between the concentration of radicals dissolved in the solution and its equilibrium partial pressure in the gas phase can be estimated from the free energy of solvation by using eq 8.[37]

$$k_H = \exp(-\Delta G_s/RT)/RT \tag{8}$$

By employing the above equations, we can obtain the ΔG_s^0 value to be −1.0 kcal/mol at 298.15 K and the k_H for ClO radical to be 5.5 M/atm. This value is much lower than that of the OH

(49) Ciccotti, G.; Ferrario, M.; Hynes, J. T.; Karpal, R. *Chem. Phys.* **1989**, *129*, 241–255.
(50) Jungwirth, P.; Tobias, D. J. *J. Phys. Chem. B* **2002**, *106*, 6361.
(51) Autrey, T.; Brown, A. K.; Camaioni, D. M.; Dupuis, M.; Foster, N. S.; Getty, A. *J. Am. Chem. Soc.* **2004**, *126*, 3680.
(52) Ben-Naim, A.; Marcus, Y. *J. Chem. Phys.* **1984**, *81*, 2016.

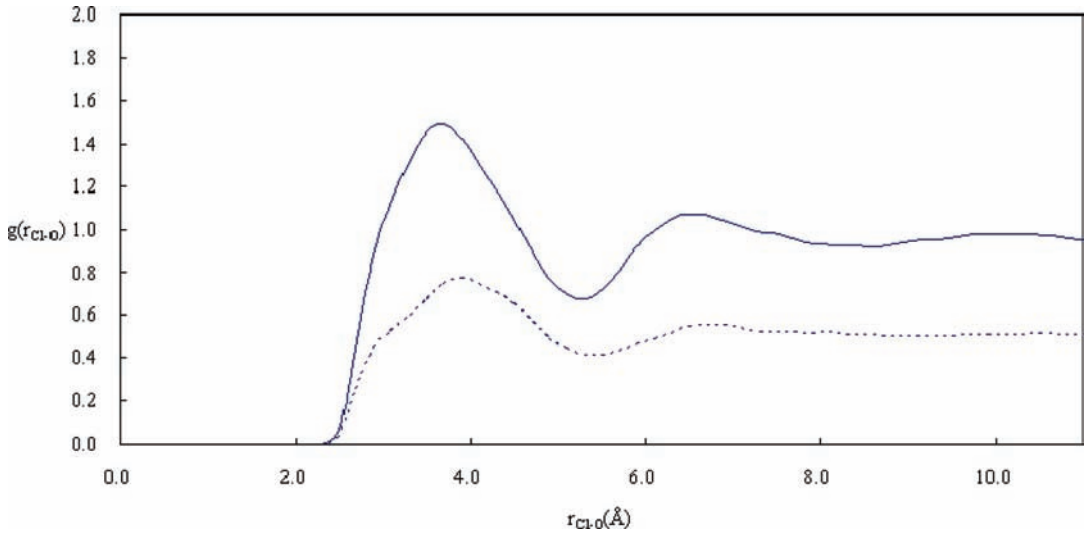

Figure 4. The Cl(O)−O(water) RDF plot of the NVT ensemble. The solid line is calculated when the ClO radical is in the center of the water bulk, and the dashed line is calculated when the ClO radical is on the air−water interface.

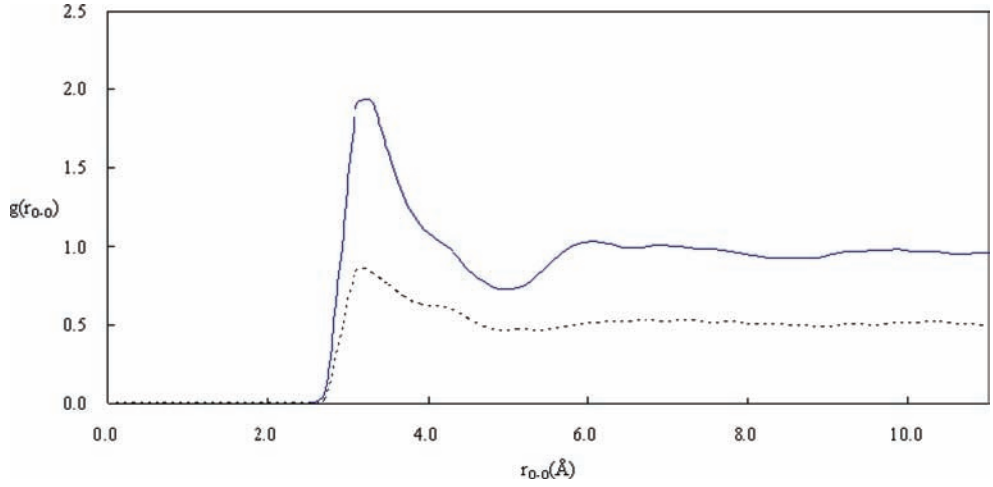

Figure 5. The O(Cl)−O(water) RDF plot of the NVT ensemble. The solid line is calculated when the ClO radical is in the center of the water bulk, and the dashed line is calculated when the ClO radical is on the air−water interface.

radical (30 M/atm),[53] which indicates that ClO dissolves less readily in water than OH radical.

Figures 4 and 5 show radial distribution functions (RDFs) water solvation of ClO for the NVT ensemble (see also Supporting Information Figures 1 and 2 for RDFs of the NPT ensemble). The first interesting distance used in $g(r)$ is the distance between the O atom in water molecules and the Cl atom in the ClO radical. The results show that the $g(r_{Cl-O})$ has a peak at a distance of $r = 3.5$ Å for the NPT ensemble as shown in Supporting Information Figure 1, which is much longer than the Cl···O hydrogen-bond distance (2.8 Å) in the global minimum of the $ClO \cdot H_2O$ complex and is close to that of the local minimum (3.5 Å) as shown in Figure 1. As to the NVT ensemble shown in Figure 4, simulations are performed for both cases of ClO inside the water bulk and ClO within a distance of 0.5 Å of the interface. These two simulations give consistent predictions of the solvation shells. The first peaks appear at $r = 3.7$ and 3.9 Å for ClO inside the bulk and ClO at the interface, respectively. These values are also consistent with the predictions of the NPT ensemble. These results imply that the O(Cl)−H(water) interaction may be stronger than the Cl−O-(water) ones, which results in the ClO radical interacting with liquid water, creating a reactive site at the Cl end because the O atom of the ClO radical is more likely to be hydrogen bound to water molecules at the interface.

We also calculated the $g(r)$ for the distance between the oxygen atom in the ClO radical and the oxygen atoms in the water molecules (r_{O-O}). As shown in Supporting Information Figure 2, the peak appears at 3.1 Å in the calculation of RDF with NPT ensemble. This distance is consistent with that in the local minimum of the $ClO \cdot H_2O$ complex shown in Figure 1, where the O−O distance is 3.0 Å at the level of CCSD(T)/aug-cc-pVTZ and is 3.1 Å with our newly parametrized mTTM potential. Note this is remarkably different from the global minimum of the $ClO \cdot H_2O$ complex, where the O−O distance is calculated to be 4.4 Å for both ab initio calculation and mTTM model in this work. We also calculated $g(r)$ for the NVT ensemble for both cases where the ClO radical is

(53) Hanson, D. R.; Burkholder, J. B.; Howard, C. J.; Ravishankara, A. R. *J. Phys. Chem.* **1992**, *96*, 4979.

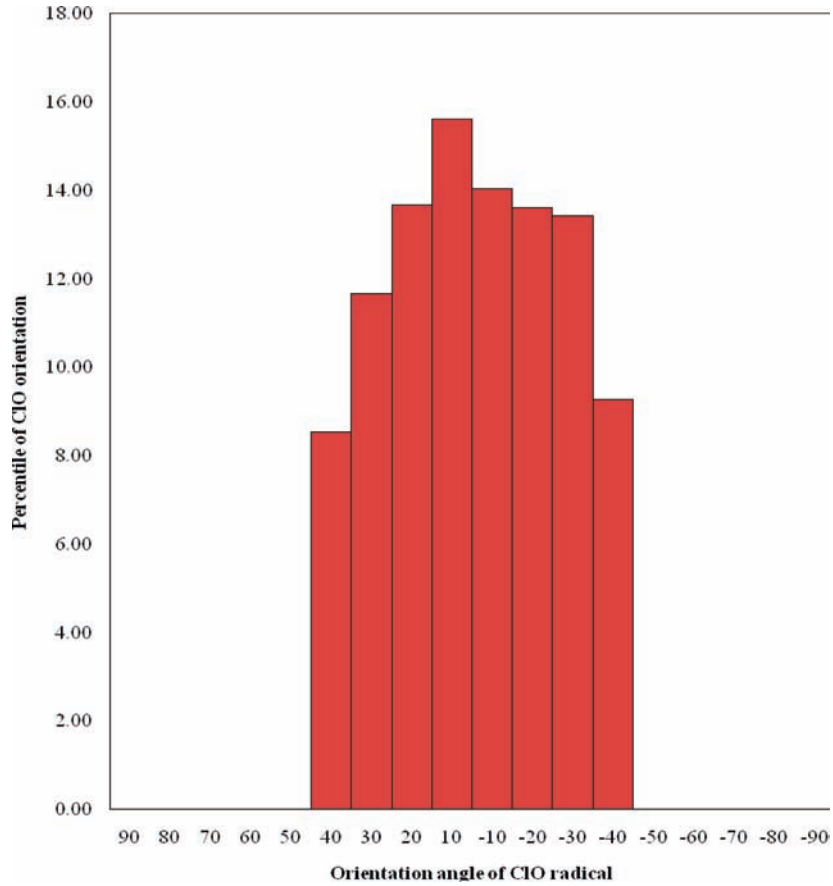

Figure 6. Histogram of ClO radical on the water surface. The angle is positive when the O atom is on the top, is negative when the Cl atom is on the top, and is zero when the ClO radical is parallel to the surface.

inside the water bulk and where the ClO radical is on the surface of the water bulk. The data are shown in Figure 5. The r_{O-O} values corresponding to the first peaks are 3.3 and 3.1 Å with the radical inside the bulk and the radical on the interface, respectively. These data are in excellent agreement with the finding of the calculations with the NPT ensemble. One may notice there is a 0.2 Å difference in the positions of r_{O-O} and r_{Cl-O} peaks between NPT ensemble and NVT ensemble with the radical dissolved inside, which may arise from the size effect of the water slab. However, this difference is small, and the bonding pattern can be quite clearly seen from the positions of r_{O-O} and r_{Cl-O} peaks, which are much closer to the local minimum than to the global minimum for both NPT and NVT ensembles, so this difference should not affect the conclusions from the RDF calculations. These simulations confirm that the most probable configuration for ClO radical accommodation in liquid water is with the ClO hydrogen bonded to water molecules from its oxygen end and not the chlorine end.

The orientation of ClO radical on the water surface is shown in Figure 6. It can be seen that the orientation of the ClO radical on the water−air interface is mostly parallel to the water surface. The snapshots with the ClO radical in the middle and on the surface of the water slab are given in Figure 7. This figure also shows the typical orientation of the ClO radical on the air−water interface with the ClO bond nearly parallel to the interface. This orientation will allow access to both ends of the molecule, but, as we show above, greater solvation of the O end will favor interactions with the Cl end. This suggests that the chlorine end of ClO radical is a more probable reactive site for reactions of ClO radical on a water surface.

The solvation structure and orientation of ClO at the water interface also suggest that another ClO from the gas phase will most probably react with the ClO radical on the water surface at the chlorine end, which would lead to the production of nascent ClOClO molecules. This result is contrasted with the gas-phase recombination reaction of ClO radicals, which only produces ClOOCl.[15,54,55] Radical−radical association reactions in the gas phase are typically barrierless, and the new molecule is formed with large excess energy, which is slowly dissipated by collisions with other gas-phase species. The long relaxation time will favor formation of the more thermodynamically stable ClOOCl molecule in the gas phase. The close proximity of solvent molecules in the liquid phase will lead to more rapid quenching of excess energy and trapping in less stable configurations, for example, ClOClO. Therefore, it is likely that in the liquid phase the branching ratio of the association reaction is kinetically determined. The solvation of the ClO radical at the interface directs the reaction to the local equilibrium structure, ClOClO, and rapid quenching traps it there. Therefore, the combination of solvation structure of ClO and rapid quenching of the nascent ClOClO species will lead to the small probability of the formation of symmetric ClOOCl molecules on the surface of liquid water.

(54) Molina, L. T.; Molina, M. J. *J. Phys. Chem.* **1987**, *91*, 433.
(55) Nickolaisen, S. L.; Friedl, R. R.; Sander, S. P. *J. Phys. Chem.* **1994**, *98*, 155.

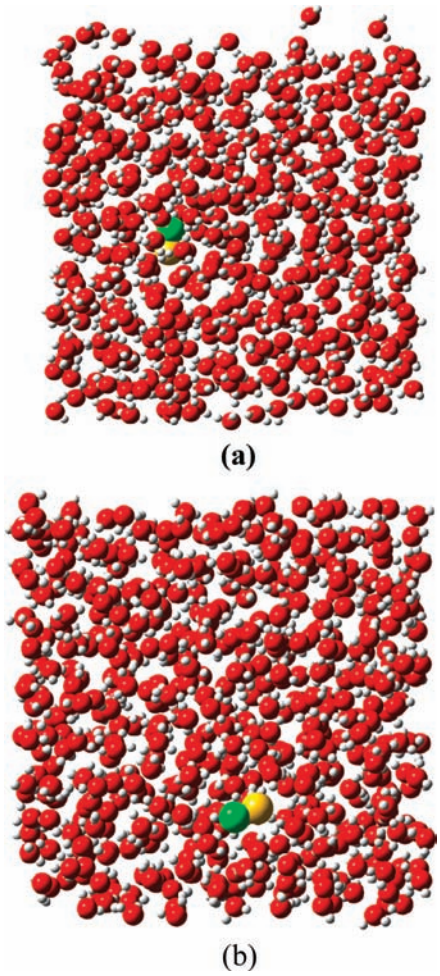

Figure 7. The snapshots of the ClO NVT simulation: (a) the side view on the configuration that the ClO radical is in the middle of the water bulk; (b) the top view on the configuration that the ClO radical is on the air−water interface.

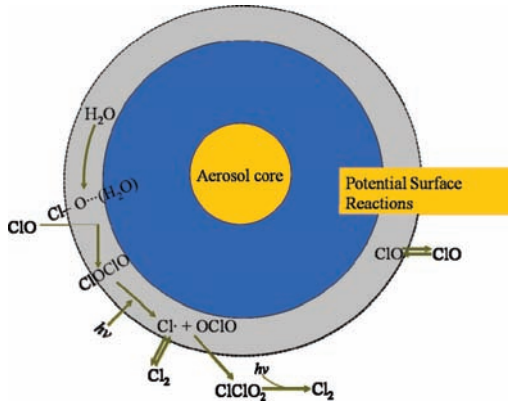

Figure 8. Schematic diagram of ClO radical chemistry at the air−water interface.

Photodissociation of ClOClO leads to the photoreaction of Cl atoms and OClO.[56] McKeachie et al.[57] found experimentally that OClO and $ClClO_2$ are generated when ClO radicals are passed over water−ice surfaces. They did not observe the production of symmetric ClOOCl molecules. Because the formation of OClO and $ClClO_2$ is reported to be generated from the ClOClO molecule according to McGrath et al.[58] shown as in eqs 9 and 10, the present calculations lead to a theoretical explanation of the previous experimental results of McKeachie et al.[57]

$$ClO + ClO + M \rightarrow ClOClO + M \quad (9)$$

$$ClOClO \rightarrow Cl + OClO \rightarrow ClClO_2 \quad (10)$$

Findings from this work suggest that liquid water can accommodate ClO radicals and change the reaction pathway of the ClO recombination. Figure 8 illustrates the proposed new interfacial chemistry of ClO radical on water surfaces. Leu et al.[45] first suggested that the heterogeneous reaction of ClO, that is, ClO surface recombination on aerosols, could be a source of Cl_2. This is consistent with the chemistry proposed in these studies. By assuming a reaction probability of 0.1 for the recombination of two ClO radicals to give Cl_2 on an aerosol surface and a gas−aerosol[59] collision frequency of 10^{-3} s^{-1}, Leu et al.[45] found that the heterogeneous uptake of ClO followed by surface recombination reactions to give Cl_2 could be a mechanism that is competitive with the ClO dimer homogeneous gas-phase reaction. Our recent study of radical recombination reactions[60] on water shows that these reactions can be quite fast (less than 2.0 ps) on water. Our findings from this work suggest that understanding the impact of a large accommodation for ClO and its subsequent chemistry in an environment with high water vapor concentration becomes important as water vapor abundances increase into the midstratosphere region where there is a high ClO number density.

IV. Conclusions

In this work, we performed classical MD simulation on the ClO radical−liquid water interaction with the mTTM and TTM2-R potentials. Our new parameters give better prediction on the geometries of the minimum in PES of $ClO\cdot H_2O$ system. The scattering simulations of ClO radical on the surface of liquid water give a direct examination of how the ClO radical is accommodated from the gas phase into the liquid phase. The mass accommodation coefficient is estimated to be 0.85 at 298.15 K. The result of the free energy profile calculation of ClO radicals on liquid water shows that the ClO radical has a higher propensity to be adsorbed onto the air−water interface rather than fully dissolved into the water bulk. The ΔG_s and ΔG_s^0 values for the ClO radical are calculated to be −2.9 and −1.0 kcal/mol, respectively, and Henry's law constant is hereby calculated to be 5.5 M/atm, lower than that of the OH radical. The RDF calculations, performed for NVT and NPT ensembles, show that the reactive site for ClO radical on a water surface is at the Cl end and the O atom of ClO is more likely to be hydrogen bound in the aqueous phase. From the calculations, it is suggested that the recombination reaction of ClO radicals may have different pathways in the presence of liquid water and in the gas phase. This is consistent with the experimental results and provides new insight into chlorine chemistry in the atmosphere.

(56) Matus, M.; Nguyen, M. T.; Dixon, D. A.; Peterson, K. A.; Francisco, J. S. *J. Phys. Chem. A* **2008**, *112*, 9623.
(57) McKeachie, J. R.; Appel, M. F.; Kirchner, U.; Schindler, R. N.; Benter, Th. *J. Phys. Chem. B* **2004**, *108*, 16786.
(58) McGrath, M. P.; Clemitshaw, K. C.; Rowland, F. S.; Hehre, W. J. *J. Phys. Chem.* **1990**, *94*, 6126.
(59) Toon, D. P.; Hamill, T.; Turco, R. P.; Pinto, J. *Geophys. Res. Lett. B* **1986**, 1284.
(60) Du, S.; Kais, S.; Francisco, J. S. *J. Chem. Phys.* **2009**, *130*, 124312.

Acknowledgment. We would like to thank Collin D. Wick and Tsun-Mei Chang for their assistance. Work by B.C.G. and G.K.S. was supported by the Chemical Sciences Division, Office of Basic Energy Sciences, Department of Energy. The Pacific Northwest National Laboratory is operated by Battelle for the U.S. Department of Energy.

Supporting Information Available: Two figures that show the radial distribution functions for the ClO radical in the liquid water slab of the NPT ensemble and complete ref 36. This material is available free of charge via the Internet at http://pubs.acs.org.

JA9033186